Experimental investigations and developing multilayer neural network models for prediction of CO_2 solubility in aqueous MDEA/PZ and MEA/MDEA/PZ blends

Tianci Li, Puttipong Tantikhajorngosol, Congning Yang and Paitoon Tontiwachwuthikul, University of Regina, Regina, Saskatchewan, Canada

Abstract: In this research, a new set of experimental data for CO_2 solubility in aqueous blended amine solvents were investigated experimentally over the CO_2 partial pressure range from 8 to 100 kPa at 40 °C and were compared with the benchmark aqueous 30 wt.% MEA solution. This work developed two multilayer neural network models named models A and B, for predicting the CO_2 solubility in various aqueous blended amine solvents including 36 wt.% MDEA + 17 wt.% PZ, 24 wt.% MDEA + 26 wt.% PZ, and 6 wt.% MEA + 25 wt.% MDEA + 17 wt.% PZ. Models A and B were developed by using Levenberg–Marquardt back propagation algorithm with 427 and 301 of reliable experimental data sets gathered from the published data, respectively. The results indicate that the high accuracy prediction of the CO_2 solubility in Methyldiethanolamine/Piperazine (MDEA/PZ) blends could be obtained by the network developed by Tan-sigmoid transfer function with two hidden layers consist of eight and four neurons, while the network developed by Tan-sigmoid transfer function with three hidden layers consist of 20, 10, and five neurons provided the highest accuracy for predicting the CO_2 solubility in MEA/MDEA/PZ blends comparing to other model structures. The comparison results show that the neural network modeling provided more closer predictions to the experimental results than the simulator and other thermodynamic models when predicting the CO_2 equilibrium solubility in blended amine solvents. © 2021 Society of Chemical Industry and John Wiley & Sons, Ltd.

Keywords: amine blends; ANN; CO_2 capture; experimental validation; model; solubility

Introduction

Carbon dioxide is one of the main greenhouse gases that can cause global warming and other environmental issues. Fossil fuels are still the major

energy contributors for current technology development and human activities. Reliable data and model predictions[1] reveal that the impact of Covid-19 pandemic accelerated energy transitions, and a significant reduction of global energy demand

occurred during the pandemic in 2020, but combustible fuels still provided more than half the amount of energy for electricity generation during 2019–2020 throughout the world. Therefore, it could be predicted that energy demand would increase once the global economy fully reopens after the pandemic. It results in higher amount of CO_2 emission being rapidly released into the atmosphere due to the combustion process of natural gas, oil, coal, and other fossil fuels. Recently, the demand of natural gas has been increasing significantly for the leading countries in energy consumption such as China, the United States, and Russia. The U.S. Energy Information Administration (EIA) forecasted that the consumption of natural gas worldwide would increase from 120 trillion cubic feet in 2012 to 203 trillion cubic feet in 2040.[2] Coal is gradually replaced by natural gas, which is helpful for energy transition because natural gas produces lesser CO_2 and fewer contaminant. However, direct CO_2 emission from natural gas combustion to the atmosphere is a factor that should not be overlooked. Consequently, fossil fuel combustion with carbon capture is an effective strategy to achieve the reduction of carbon emission and this technology plays a key role in transition to carbon neutrality.

There are three typical carbon capture techniques, including oxyfuel technology, precombustion technology, and postcombustion technology (PCC). Among these techniques, PCC is considered the most mature process since it is efficiently applicable to most large-scale existing fossil fuel power plants and cement plants. The success of Boundary Dam Integrated CCS Demonstration and PetraNova Project confirmed that postcombustion technology is an effective approach for reducing carbon emissions.[3] PCC is also acceptable to be utilized for natural gas combined cycle plants (NGCC). Several companies and organizations have started or proposed their commercial-scale project combining natural gas power plant with PCC technology, such as the Karsto NGCC Capture Project by the Norwegian government, Nanko Natural Gas Pilot Plant by Kansai Electric Company, and Petershead Project in Scotland. Furthermore, it was reported by Global CCS Institute in 2020[4] that there are 65 commercial CCS facilities in various stages of development throughout the world and the global capture and storage capacity has increased by 33% since 2019.

Amine-based chemical absorption is a mature technology, which has been widely applied on the postcombustion process for decades. Chemical absorption aims to absorb the CO_2 from a flue gas by using several chemical solvents. Traditionally, single amine-based solvents can be categorized as primary amines, secondary amines, tertiary amines, primary sterically hindered amines, and polyamines. Monoethanolamine (MEA) is a typical primary amine utilized in current commercial-scale postcombustion process as a benchmark solvent since it provides a fast reaction rate with CO_2.[5] However, there are some significant limitations of MEA negatively affecting the operating costs, including low absorption capacity, high corrosion risk, high vaporization losses, and high regeneration energy consumption.[6–8] In other words, each type of amine has its own advantages and various potential drawbacks. The drawbacks of the single solvent restrict its further operation performance in CO_2 capture technology. The performance of the solvent will be graded more strictly once the operation conditions are more complicated and challengeable. For instance, the flue gas from natural gas power plants has conceptually lower CO_2 content, which causes higher challenge on the absorption process in comparison to that from a coal-fired power plant. Therefore, developing more efficient solvents is a promising strategy to improve the CO_2 capture technology. Desired solvents should involve several features such as high absorption capacity, fast CO_2 absorption rate and low regeneration heat.[9,10]

In the past few years, the performance of the amine solvents has been continuously upgraded with the appearance of new generation solvents. Blended amine solvent leads a new trend of solvent development, which has attracted attention due to its considerable benefits.[11] The main objective of using blended amine solvent is to improve the absorption performance in the meantime to reduce regeneration heat consumption in stripper. Current published papers compared single tertiary amine and blended amine solvents[11–16] and stated that those blended amine solvents, which were composed of one bicarbonate forming amine solvent and one (or more) carbamate forming amine solvent, can provide enhanced absorption performance, better mass transfer performance, and higher absorption capacity. MEA and piperazine (PZ) are two typical carbamate forming amine solvents that could be utilized to activate the low reactive solvents.[11] Methyldiethanolamine (MDEA) is a tertiary amine, which has a larger CO_2 absorption capacity but is less reactive with CO_2 since it cannot

form any carbamate.[17] Therefore, single MDEA is not a proper solvent for the CO_2 capture process at low pressure operations. However, high CO_2 absorption capacity with less regeneration energy requirement, lower corrosivity, and relatively lower unit price are the leading advantages attracting researchers to explore the new generation blended amine solvent using MDEA as the base solvent.

Bishnoi *et al*.[18] investigated the solubility of CO_2 in various concentrations of the PZ solutions under different CO_2 partial pressures at temperatures of 313 and 343 K. They have studied the early-stage investigations for the effect of pressure and temperature on the CO_2 solubility in single PZ solvent since 2000. Several researchers[12,19] later reported that the CO_2 solubility in PZ is normally higher than that in MDEA and MEA. Recently, several publications reported the utilizations of PZ as an effective activator with large CO_2 absorption capacity. Consequently, MDEA/PZ blends contribute higher equilibrium CO_2 solubility with faster CO_2 absorption rate at different range of temperatures and CO_2 partial pressure compared to other alternative amine systems, such as MEA/MDEA and single MEA solvent.[20–26] Based on those reliable experimental results, thermodynamics models were developed to correlate and predict CO_2 solubility in various blended amine solvents upon given temperature, pressure, and desired amine concentration. In the meantime, the influence of the interactions between ion pairs and MDEA or PZ molecular species were studied by several researchers.[11–13] Nevertheless, the health hazard issue and potential deposition issue of PZ could also be considered in practical industrial applications when using high concentration PZ. Hence, this research is going to replace a partial amount of PZ by MEA to form tri-solvent blends (blending three amine solvents), which is another type of blending method. For noncatalyst system, the studies of tri-solvent blends are relatively newer than single and bi-solvents. Several tri-solvent blends such as MEA/PZ/AMP and MDEA/DETA/AMP have been intensively studied by the authors.[10] Their works confirmed the excellent CO_2 absorption performance using MEA and PZ in a tri-solvent system with less regeneration heat duty compared to the single solvent 30 wt.% MEA. Most current publications related to the tri-solvent are focused on the investigations of regeneration energy demand. However, it is essential to determine the maximum absorption capacity for a specific novel

solvent because the higher absorption capacity can potentially reduce solvent and regeneration energy demands.

CO_2 solubility is defined as a physical property of solvent that can be used to estimate the absorption capacity, the measurement of CO_2 solubility is a fundamental work for the researchers who are willing to develop new solvents. The experiment methods can be categorized as closed-open circuit methods, analytical methods, and synthetic methods.[19–26] The influencing factors of CO_2 solubility for one specific solvent are the effect of temperature, the effect of CO_2 partial pressure, the effect of amine type, and amine concentration. However, managing laboratory experiments is usually time-consuming, energy-consuming, and chemicals-consuming, particularly the experiments under high pressure and temperature. In addition, its calculation using correlations is complex and does not perfectly cover the wide ranges of temperature, pressure, and concentration due to the limitation of the correlations. Thus, many researchers attempt to use AI technology based on several machine learning algorithms as predicting tools to estimate CO_2 solubility.

The artificial neural network (ANN) is a typical machine learning algorithm; it can be a nonlinear predicting tool that imitates human brain, which is composed by the connections of neurons. It can efficiently predict the physical properties of solvents in CO_2 capture process due to the nonlinear relationship between the input data and the output data.[13] Therefore, ANN models can efficiently cover both low to high temperature and partial pressure region based on extensive input data.

The ANN models were established upon the experimental data of CO_2 equilibrium solubility for aqueous MDEA/PZ and MEA/MDEA/PZ blends, which improved the prediction accuracy. Equilibrium data of CO_2 solubility at wide ranges of temperature and pressure in several amine solutions are indispensable for improving the prediction accuracy of the ANN models. In recent years, ANN systems were widely studied as a tool to predict the solvent properties.[26–30] Hamzehie *et al*.[31] suggested that feed-forward multilayer network was an efficient method to predict the CO_2 solubility in aqueous amine blends. The feed-forward neural network was one of the main networks in ANN technology, which was computed based on back-propagation learning algorithm and multilayer perceptron driven

approach.[32,33] However, there are no specialized studies focusing on the predictions of CO_2 solubility in MEA/MDEA/PZ blends with ANN method. Meanwhile, the experimental investigations of the tri-solvent for CO_2 solubility are lacking, especially at specific high concentrations of PZ, hence the experimental works of this present research are essential to develop the ANN model for predicting CO_2 solubility in MEA/MDEA/PZ blends.

In this work, CO_2 solubilities were investigated experimentally at several CO_2 partial pressure, and two ANN models were employed to predict the CO_2 solubility in aqueous MDEA/PZ and MEA/MDEA/PZ, respectively. A comparison between ANN and other prediction tools (several thermodynamics models and simulated results from ProMax 5.0) were studied in this paper. The implementations of two back-propagation neural network ANN models were developed named as models A and B through MATLAB Neural Network Toolbox. Model A was the prediction model for the CO_2 solubility in MDEA/PZ solvent, while model B was developed to predict the CO_2 solubility in MEA/MDEA/PZ solvent.

Methodology

Experimental section

Chemicals

Deionized water; MEA ($\geq$ 98%), MDEA ($\geq$ 99%), PZ ($\geq$ 99%) purchased from Sigma-Aldrich; 8, 15.1, 30, 50, and 100 vol.% CO_2 (N_2 balanced) gas cylinders were supplied by Praxair Inc., Canada.; hydrochloric acid (HCl) was purchased from Fisher Chemical (USA).

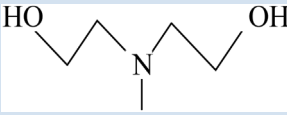### Amine structure

The following amines used for this research were MEA, MDEA, and PZ. The chemical structures for these amines are listed in Table 1.

Measurements

A schematic drawing of the CO_2 solubility apparatus is shown as Fig. 1. The amine reactor was placed inside of the silicone oil heating bath (The PolyScience PD Performance Digital 7L Heat Bath; Cole-Parmer, Canada), which was specified to 40 °C. The dry feed gas (8–100 vol.% CO_2 with N_2 balanced) was introduced to the water saturator (100 mL), then the saturated gas was introduced to the amine reactor to react with the solvent (30 mL). The IR (Infrared detector) analyzer

Table 1. Chemical structures.

Name	Chemical structure
Monoethanolamine (MEA)	
Methyldiethanolamine (MDEA)	
Piperazine (PZ)	

Figure 1. Schematic of CO_2 solubility apparatus.
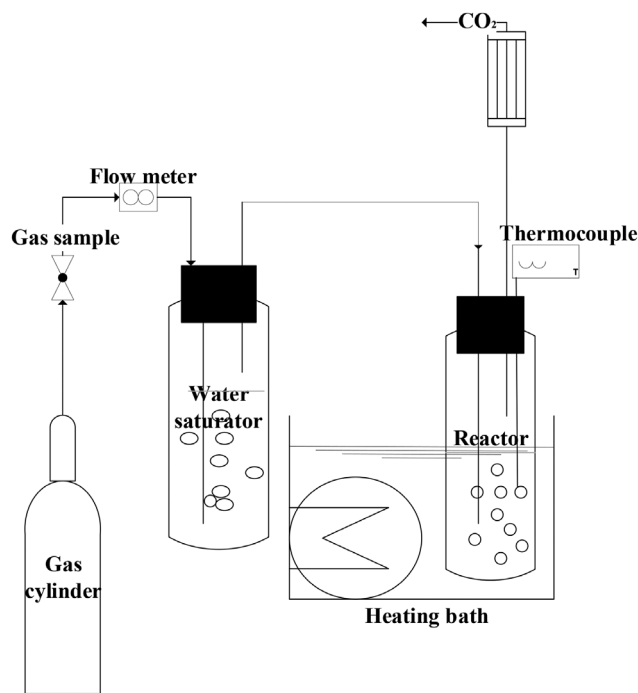
(NOVA Analytical System Inc., USA) was manually calibrated the gases with approximately 1% of the relative standard uncertainty to ensure the desired CO_2 partial pressure in the feed gas was applied. To ensure the feed gas fully interacted with the solvent, the proper gas flow rate (0.5 $\pm$ 0.01 SLPM) was controlled by the needle valve and monitored by the digital gas

flow meter (EW-32908-73; Cole-Parmer). Through the experiment, it was found that high gas flow rate could remove a partial amount of water from the amine solution and changing the solvent composition. It takes at least 6 hr of the duration to achieve the equilibrium loading for one trial. The measurement of CO_2 loading at equilibrium was repeated twice and the average taken at a time interval of half hour after 6 hr. The CO_2 loading measurement was completed using the Chittick apparatus to titrate the specific volume of solvent sample with a standard 1 M hydrochloric acid and using 0.1 wt.% methyl orange solutions as a color indicator. The equilibrium was achieved when the latest reading of CO_2 loading was extremely close to the previous reading of CO_2 loading. To be specific, the difference between two consecutive readings of CO_2 loading should be less than 3%. This empirical value was taken from the average deviation between the two readings of CO_2 loading at each interval. To enhance the accuracy of the experimental data, a condenser was connected to the gas outlet of the amine reactor. It is known that the unreacted gas could contain a small amount of vaporized amine, hence vaporization losses can be avoided by the condensation process. The cooling water (8 °C) in the condenser was circulated by using the circulating chiller (Isotemp, Fisher Scientific, Canada). The condensed amine was returned to the amine reactor after condensation to maintain the identical volume of amine solvent in the reactor. For the experiment, the CO_2 solubility in 5 M MEA was tested firstly to valid the experimental data by comparing with other published data, which would be discussed in the next section.

Artificial neural network section
Basic description

ANN technique is a unique predicting tool since it is a nonparametric statistical modeling tool with large capability to process the data from extended database.[31–33] In the past 20 years, researchers have developed several mathematical models to predict the physical properties.[34–38] Traditionally, the vapor–liquid equilibrium (VLE) of CO_2-amine system is typically considered as the basic theory for correlating and predicting the solubility data. Thus, a number of thermodynamic models were employed used for correlating and predicting the CO_2-amine system such as Deshmukh–Mather model, Pitzer's excess Gibbs energy-based models, electrolyte nonrandom

two-liquid [e-NRTL]model, Kent–Eisenberg model, extended UNIQUAC model and extended Debye–Hückel theory applied to long-range ion-ion interactions.[12,13] Recently, neural networks have been widely studied and used in CO_2 capture process for predicting physical properties of the solvents and other purposes. Fotoohi *et al.*[39] evaluated pure and binary gas adsorptions on activated carbon as the absorbent by using different two-dimensional equations of state including Redlich–Kwong (RK), Soave—Redlich–Kwong (SRK), Peng–Robinson (PR), modified Mohsennia–Modarress–Mansoori (M4), and ANN method. The results indicated that the ANN model predicted the adsorption with more accurate results than other equations of state. Garg *et al.*[40] investigated the CO_2 solubility in aqueous sodium salt of ʟ-phenylalanine experimentally and correlating them with the prediction results by using the modified Kent–Eisenberg and ANN model. They also indicated that the average deviation between ANN and experimental data is only 2.99%, which is significantly lower than the average deviation between the prediction results from the modified Kent–Eisenberg model and experimental data. Baghban *et al.*[41] developed a multilayer perceptron ANN and an adaptive neuro-fuzzy interference system to predict CO_2 solubility in presence of various ionic liquids over wide range of temperature, pressure, and concentration. They also mentioned that multilayer perceptron ANN provided better agreement for predicting CO_2 solubility based on statistical criteria. For amine-CO_2 system, Fu *et al.*[42] analyzed the mass transfer performance when using MEA-based solvent in a packed column and they also confirmed that ANN models are suitable in predicting mass transfer performance for CO_2 capture process. Two ANN models were developed by Pouryousefi *et al.*[43] in order to predict and correlate physical and heat transport properties of the solvent, including density, viscosity, refractive index, heat capacity, thermal conductivity, and thermal diffusivity. They affirmed that both back propagation neural network and radial basis neural network can predict the properties with higher accuracy than the predictions of empirical model. The back-propagation neural network has been successfully developed and employed to correlate and predict the CO_2 equilibrium solubility in seven tertiary amines by the researchers.[9,44]

Chen *et al.*[44] evaluated the prediction performance of CO_2 solubility in 12 known amine solutions by using

back-propagation neural networks (BPNN) and radial basis function neural networks (RBFNN). They also discussed the possible reason of why BPNN models performs better than the RBFNN models for predicting the CO_2 solubility, it is because that the characteristics of the error back propagation of BPNN models, the adjustment of initially generated weights and biases can efficiency retraining the network to the desired error which is a way to improve the prediction accuracy.[44] Hamzehie *et al*.[45] compared various architectures of neural network models with two hidden layers and different number of neurons for the predictions of CO_2 solubility in various aqueous blended amines. The result indicated the optimal network architecture was trained by the Levenberg–Marquardt back-propagation algorithm and the Gauss–Newton method with combination of a Bayesian regularization technique consists of two hidden layers containing eight and four neurons in the first and second layer, respectively. The hidden layers and neurons were active by using tan sigmoid function, which have been confirmed as a high effective approach by Hamzehie *et al*.[45] and Golzar *et al*.[46] Therefore, it is challenging and benefits to apply ANN to predict CO_2 solubility in blended amine solvent.

It should be noticed that the output data (a) is generally obtained through the computing system with different transfer functions. Essentially, the summation of the biases (b_i) and the product of different input data (p_i) and its weight (w_i) are computed through the hidden layers and transferred to the output layer by using the desired transfer function, so it can be concluded as the equation below:

$$a = f\left(\sum_{i=1}^{N} w_i p_i + b_i\right) \tag{1}$$

In this study, the input parameters of model A consist of the total amine concentration (X_{amine}), temperature (T), CO_2 partial pressure (P) and molecule weight (MWa), this structure can efficiently help the system understand the composition of the solvent. Model B is applied to correlate and predict the CO_2 solubility in aqueous tri-solvent MEA/MDEA/PZ blends at 40 °C, and the weight fraction of MEA (X_{MDEA}), MDEA (X_{MDEA}), and PZ (X_{PZ}) are employed as the input data instead of the total amine concentration (X_{amine}). According to the Eqn (1), the function of models A and B can be defined as Eqns (2) and (3), respectively, as follows:

$$\alpha_{CO_2} = f(X_{amine},\ MWa,\ T,\ P) \tag{2}$$

$$\alpha_{CO_2} = f(X_{MEA}, X_{MDEA}, X_{PZ},\ MWa,\ P) \tag{3}$$

where α_{CO_2} represents the CO_2 loadings.

General ANN model development

It is well known that the data distributions are strongly influenced by data collection.[44] Typically, the process of constructing the ANN models can be categorized into six steps. These steps are the (1) data collection, (2) data normalization, (3) network configuration determination, (4) processing data, (5) error analysis, and (6) adjusting weight and bias if the error is unacceptable or ending if the error is acceptable. In general, the collected data points were normalized before sending them to the system by using following equation:

$$Y_i = \frac{(X_i - X_{min})}{(X_{max} - X_{min})} \tag{4}$$

where Y_i represents the normalized training and testing data sets; X_i represents the training and testing data sets; X_{min} and X_{max} are represents the minimum and the maximum values of variable.

Typically, there are three transfer functions applied to multilayer neural networks, including Log–Sigmoid transfer function (logsig), Tan–Sigmoid transfer function (tansig), and linear transfer function (purlin) as shown in Fig. 2. Activation functions can directly transform the information from the front layer to the next layer and computes the weighted sum of input and biases. It is known that nonlinear transfer functions provide nonlinear relationships to connect input parameters with output vectors, and linear transfer function is usually used for function fitting problems for the sigmoid output neurons. The mathematical representations were summarized by Dorofki *et al*.[47] as following equations:

$$a = \text{logsig}(n) = \frac{1}{1 + e^{-n}} \tag{5}$$

$$a = \text{tansig}(n) = \frac{2}{1 + e^{-2n}} - 1 \tag{6}$$

$$a = \text{logsig}(n) = \text{purelin}(n) \tag{7}$$

A comparison between tansig and logsig was studied in this present paper to obtain the optimum transfer function employed in the ANN models of this work. According to the studies and suggestions from
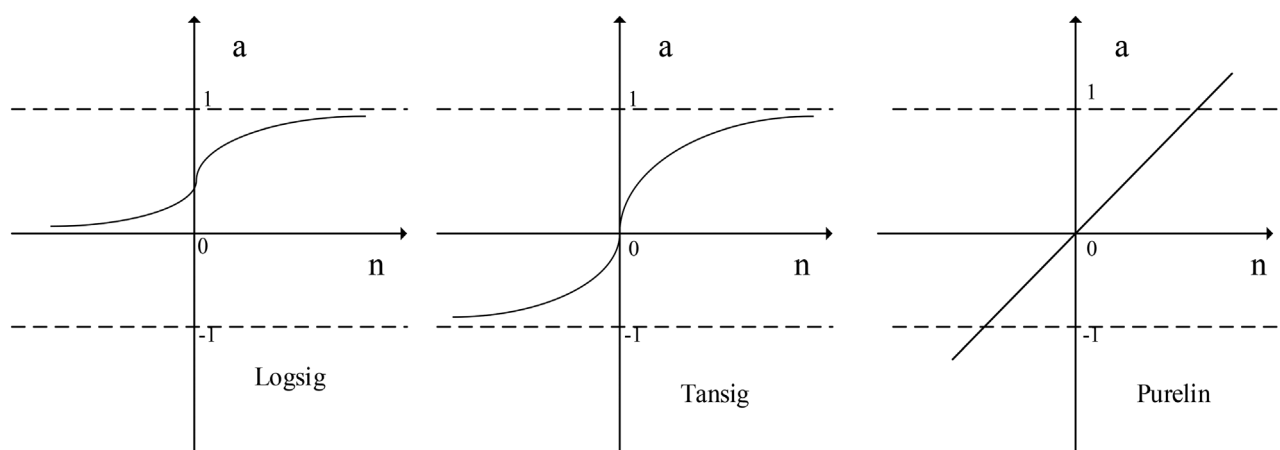
Figure 2. Transfer functions. Modified after Dorofki *et al.*[47]

Table 2. Data collection from literatures for ANN model of MDEA/PZ.						
References	T(K)	X(wt.%)	Pco_2(kPa)	MWa (g mol^{-1})	α(molco$_2$/mol solution)	No. of data points
Liu et al.[21]	303–363	19.2–60.98	13.16–935.3	21.92–71.17	0.147–0.955	80
Khan et al.[22]	303–333	33	200–4978	38.331	0.66–2.06	20
Inoue et al.[23]	313–393	10.0–50	10–100.0	8.61–56.28	0.59–1.45	9
Ali et al.[24]	313–353	22.3–23.8	0.06–95.61	26.37–28.42	0.05–0.86	59
Dash et al.[25]	303–333	30–50	0.0896–1368	33.1–59.6	0.044–1.24	259

Hamzehie *et al.*[31], the structure of model A was maintained by two hidden layers consisted of eight and four neurons, which was validated in a good agreement compared to a set of reliable experimental data. MATLAB was utilized to build the models via the neural network toolbox. All models were set and trained below 3000 of interaction (epochs) and 10^{-7} of minimum gradient, then reverting weights to reinitialize the edited weights and biases to new initial values. The models were continuously trained until the error no longer changed significantly. The desired models were able to help researchers to obtain the predictions with the minimum error percentage.

Several researchers proposed the experimental data of CO_2 solubility in aqueous MDEA/PZ solvents shown as Table 2.[21-25] These data were used as the input parameters for training the model A. In contrast, the knowledge gap was the lack of published work on the CO_2 solubility in aqueous MEA/MDEA/PZ blends. Zhang *et al.*[20] published the reliable experimental data of CO_2 solubility in aqueous MEA/MDEA/PZ blends, but the amount of their experimental data was deficient for training the ANN model. Hence, a number of input data for model B were collected from the reliable

experimental data of CO_2 solubility in aqueous bisolvents was shown in Table 3, such as MEA/MDEA and MDEA/PZ in order to improve the prediction accuracy.[18,23,25,48-52] Besides, to ensure the network structure is acceptable and effective, the mean square errors (MSE), the mean relative errors (MRE), and the correlation coefficient (R^2) are proposed to validate the prediction accuracy of the neural network model. The MSE and the MRE are defined as following equations:

$$\text{MSE} = \frac{1}{N} \sum_{i=1}^{N} \left(\alpha^{\text{exp}} - \alpha^{\text{predicts}} \right)^2 \tag{8}$$

$$\text{MRE} = \frac{1}{N} \sum_{i=1}^{N} \frac{\text{Abs} \left(\alpha^{\text{exp}} - \alpha^{\text{predicts}} \right)}{\left(\alpha^{exp} \right)} \times 100 \tag{9}$$

$$R^2 = 1 - \frac{\sum_{i=1}^{N} \left(\alpha^{\text{predicts}} - \alpha^{\text{exp}} \right)^2}{\sum_{i=1}^{N} \left(\alpha^{\text{exp}} - \bar{\alpha}^{\text{exp}} \right)^2} \tag{10}$$

where N is the total number of data points; α^{exp} is the experimental result of CO_2 loading; $\alpha^{predicts}$ is the prediction results of CO_2 loading; $\bar{\alpha}^{exp}$ represents the mean of the experimental CO_2 loading.

Table 3. Data collection from literatures for ANN model of MEA/MDEA/PZ.

References	X_{MEA} (wt.%)	X_{MDEA} (wt.%)	X_{PZ} (wt.%)	P_{CO_2} (kPa)	MWa (g mol^{-1})	α (mol$_{CO_2}$/mol solution)	No. of data points
Derks[51]	0	6–48	5.2–13.4	0.45–98.8	18.9–61.7	0.123–0.936	30
Zhang et al.[20]	18–18.6	18–29.8	4.3–13.1	15.1	49.9–52.5	0.429–0.501	3
Inoue et al.[23]	0	0.0–40	10	10	10.0–50	0.4–0.8	5
Dash et al.[25]	0	22–30	0–8	0.18–426.1	33.1–35.4	0.12–1.4	33
Shen et al.[48]	12.0–30	0–30	0	1.0–2550	30–30.5	0.244–1.1	62
Aronu et al.[49]	15–45	0	0	0.0016–16	15–45	0.102–0.565	48
Dang.[50]	23–30	0	0–10.7	0.02–0.768	18–23.8	0.299–0.47	3
Singh.[52]	3.1–16	0	0	0.88–39.48	1.9–9.6	0.49–0.76	10
Kadiwala et al.[53]	30	0	2.6–10.8	110–6489	2.3–18.3	0.62–2.77	37
Hamidi et al.[54]	7.7–30	0–0.15	0	25–100	22–30	0.57–0.77	9
Huang et al.[55]	0	25–90	8.8–18	0.3–100	44–118	0.005–0.7	42
Ermatchkov [56]	0	0	8.8–24.9	0.115–48-.4	7.6–21.5	0.48–0.84	19
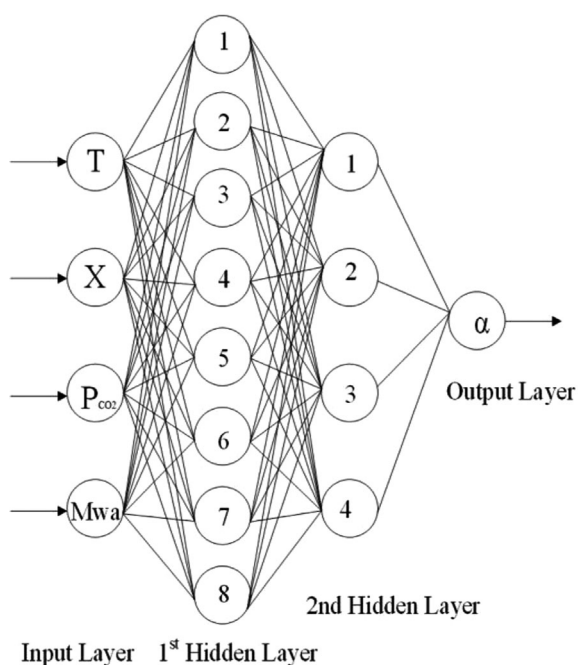
Figure 3. Structure of model A.

Development of Model A

In this research, over 400 data points[21–25,51] were used to train model A and 45 of data sets reported by Derks[51] were used to validate the model A. The maximum and minimum parameters were all normalized and listed in Table 2. Figure 3 shows the structure of the model A consisting of input layer, two hidden layers, and output layer. Nonlinear transfer function was employed for two hidden layers and a linear transfer function was only applied in the output layer.

Development of Model B

There were 301 groups of date sets used to train the model B. [19,20,23,25,48–56] Unlike the model A, the knowledge gap of the model B is the lack of reliable publications on the CO_2 solubility in aqueous MEA/MDEA/PZ blends. Thus, the data used to train the model B were not only obtained from the published experimental data related to the CO_2 solubility in aqueous MEA/MDEA/PZ, but also composed of the reliable experimental data related to the CO_2 solubility in aqueous bi-solvent, such as, MEA/MDEA blends, MDEA/PZ blends, MEA/PZ blends. To simplify the computing system, model B was computed based on the reliable data points at 40 °C only. The maximum and minimum parameters for the model B were all normalized and listed in Table 3 including various weight fraction and molecular weight of the amine under different CO_2 partial pressure and temperature. There are no similar published works that studied the same input parameters for the predictions of CO_2 solubility in aqueous MEA/MDEA/PZ blends specifically. Hence, the authors of this present work deeply analyzed different arithmetic of ANN models.

In this research, it was observed that three hidden layers with five input parameters for tri-solvent have higher prediction accuracy. One of the possible reasons

found was that the total mass concentration and the total molar concentration for some of the tri-solvent solutions are extremely close, respectively. For example, the total mass amine concentrations and the total molar concentrations of both 6 wt.% MEA + 25 wt.% MDEA + 17 wt.% PZ and 8 wt.% MEA + 30 wt.% MDEA + 10 wt.% PZ are 48 wt.% and 5 kmol m^{-1}, respectively,[3] which causes the normalized values for these two solvents are very closed to each other. At the same time, the normalized apparent molecular weight for them is extremely close as well. In this case, splitting the total amine concentration to weight fraction of MEA, MDEA, and PZ can assist the computing system to detect the composition of the amine with higher prediction accuracy for tri-solvents. This phenomenon is likely caused by the learning strategies of the ANN, process data is normally sequentially passed through all the neurons before sending it to the next layer. Unlike tri-solvents, the total molar concentration of the aqueous bi-solvent solutions in this study are the same, but the total mass concentrations are different due to their different molecular weight. The similar model configuration was studied by Golzer *et al*.,[46] they confirmed that the most appropriate transfer function and the learning algorithm employed to predict CO_2 solubility for blended amine solvents were tansig plus Levenberg–Marquardt back-propagation, and the desired input parameters consisted of individual weight fraction of the amine component and pressure. According to the identification by Hamzehie *et al*.,[45] the proper network structure should contain two hidden layers when using four input parameters. In this case, the network structure for the model B was trained at two hidden layers contains eight and four neurons first. Furthermore, 40 data points were randomly selected from the published experimental data to validate the model architecture. Those data points consist of various investigated CO_2 solubility in MDEA/PZ, MEA/PZ, and MEA/MDEA at 40 °C.[34–36,51] Table 4 provided a comparison of the correlation coefficient of training and testing for various hidden layers and neuron distributions, the reliability of the model structure would be ensured to a certain extent by comparing the correlation coefficients. The neuron network training and testing regressions were all computed from MATLAB, which was worked based on Tan–Sigmoid transfer function, a comparison between tansig and logsig transfer function was discussed in next section. As a result, a network as shown in Fig. 4 with three hidden layers

Table 4. Comparison of correlation coefficients of model B.

Network structure (Hidden layer #1- # 2- # 3)	R* (Training)	Epoch (Number of iteration)	R* (Testing)
8-4-0	0.87197	1813	0.92973
10-5-0	0.87854	1978	0.93512
15-5-0	0.91256	1946	0.93504
20-10-0	0.93502	1886	0.92886
10-5-3	0.90390	1789	0.90249
15-10-5	0.94868	1426	0.93141
20-10-5	0.98953	1103	0.97884
25-5-3	0.97891	1841	0.93789
20-15-5	0.98013	2731	0.96013
20-10-5	0.98028	2033	0.96394

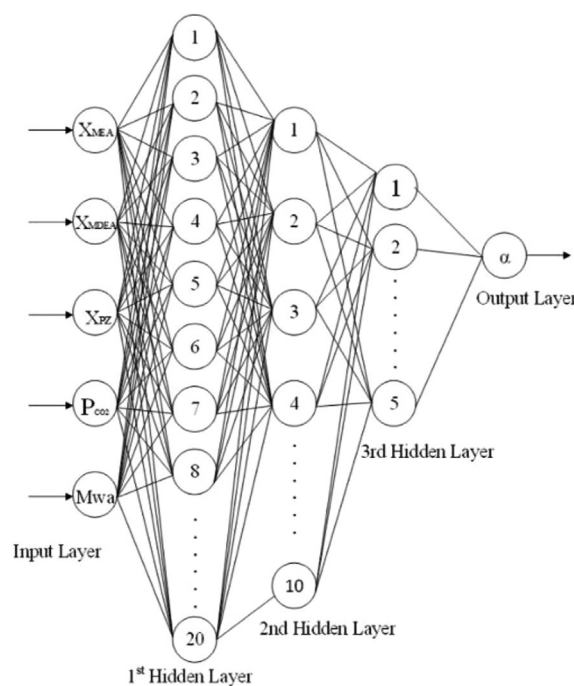*Neuron network training/testing regression (Computed from MATLAB)

Figure 4. Structure of model B.

using 20, 10, and 5 neurons in the first, second and third layer, respectively, which provides the best prediction performance for model B. Similar to model A, the input data were transported from input layer to the third hidden layer by nonlinear transfer functions,
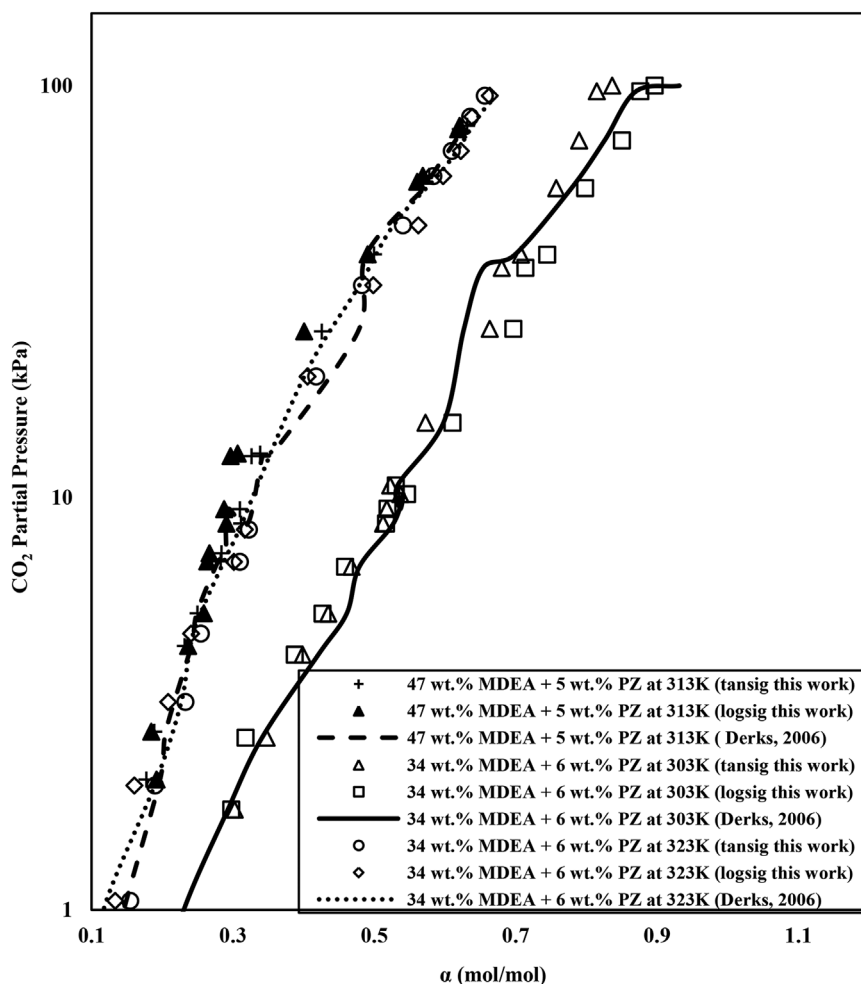
Figure 5. Performances of various training functions for model A with logsig function and tansig function.

while the linear transfer function was only applied in the output layer.

Results and discussion

Network configuration

Generally, it is impossible to analytically calculate the optimal number of layers or the number of nodes to be applied per layer in ANN models. Similarly, there is no analytical tool to calculate the optimal nonlinear activation function, it is required to validate and filtrate the optimal activation function and the structure for the desired model.

As Figs. 5 and 6 indicated above, there are two types of feedforward neural networks were computed based on two types of transfer functions transformed in the multiple hidden layers involving tansig and logsig functions. In this work, the average deviation

percentage (AAD%) was used to estimate the difference between the experimental results from this work and the modeling results or the published experimental data. The lower AAD% represents the higher prediction accuracy normally.

$$\mathrm{AAD\%} = \frac{1}{n} \sum_{i=1}^{n} \mathrm{ABS}\left(\frac{\alpha_{\mathrm{exp}} - \alpha_i}{\alpha_{\mathrm{exp}}}\right) \times 100\% \quad (11)$$

where n represents the amount of collected loadings; α_{exp} represents the loading obtained from experiment; α_i can be the loading collected from either the literature works or modeling.

The experimental data of Fig. 5 were all obtained from the investigation of Derks.[19] It can be found that the AADs when using tansig and logsig are 3.4 and 3.92%, respectively. Both two transfer functions predicted the CO_2 solubility with high accuracy, the
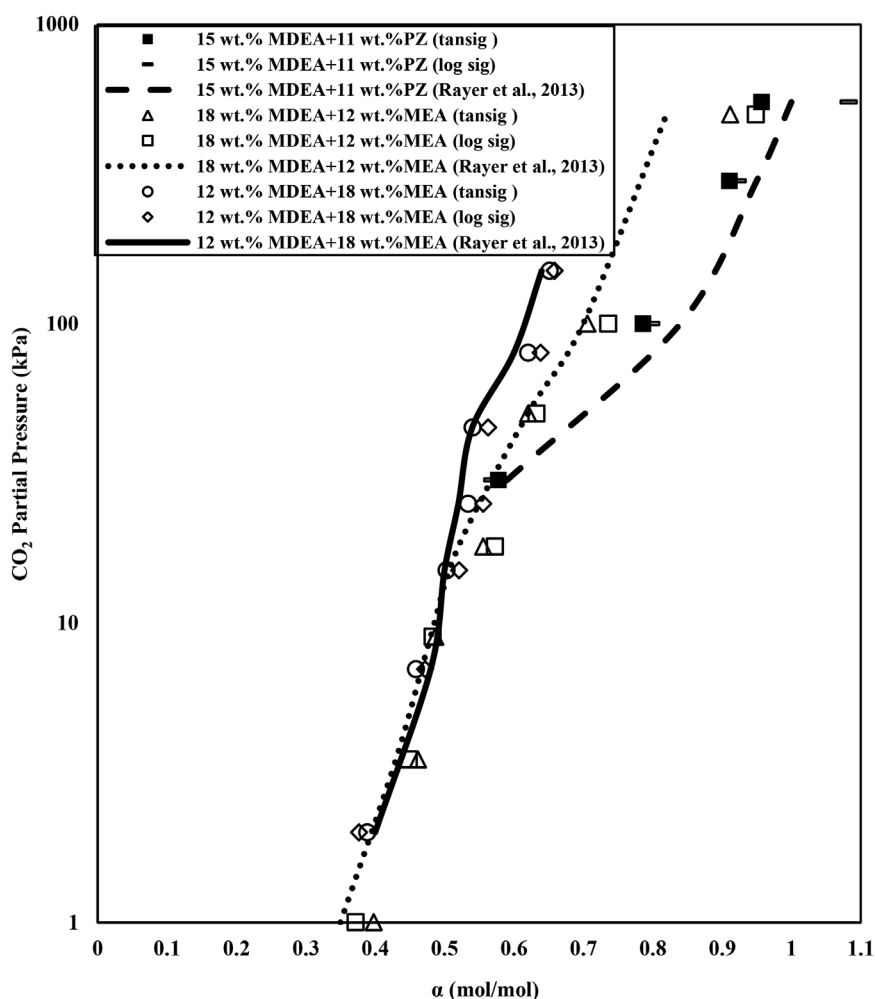
Figure 6. Performances of various training functions for model B with logsig function and tansig function.

AAD% of using tansig is slightly lower than using logsig, meaning that tansig provided better prediction results than logsig for model A. Besides, it can be observed from the MATLAB, the training regression (R) of model A achieved 0.9937 and the testing regression of model A is 0.96515 with 1089 iterations of epochs when using tansig transfer function. Therefore, it can be found that the model developed by tansig consists of two hidden layers including eight and four hidden neurons provides a good prediction results of CO_2 solubility in aqueous MDEA/PZ blends. The weights and biases of for model A were provided as Tables 5 and 6.

Comparing model B's prediction results to the experimental results[12] from Fig. 6, the network with the tansig function occurs lower AAD% than the network with logsig function again. To be specific, the

Table 5. Weights and biases of model A for the first hidden layer.

Number of the neuron on the 1st hidden layer	Weight				Biases
	T	X	P_{CO_2}	MWa	
1	2.1475	−0.2791	−3.0333	0.1245	−2.5576
2	−3.0756	2.6939	−0.5467	−0.0914	−0.0539
3	−1.2982	−0.4122	1.3164	3.6881	1.2064
4	−3.0060	2.15382	6.2022	−4.3966	3.5854
5	1.2382	−0.7863	0.2844	−0.7979	0.2881
6	0.8765	0.2453	10.2096	0.4768	11.9795
7	−0.9052	−1.2195	−3.5109	−13.6887	3.9217
8	6.2531	3.3591	1.0478	0.02388	6.7132

Table 6. Weights and biases of model A for the second hidden layer and output layer.

Number of the neuron on the 2nd hidden layer	Weight									Weight	
	Number of the neuron on the 1st hidden layer									Output layer	
	1	2	3	4	5	6	7	8	Biases	α	Biases
1	2.3902	2.1768	0.4353	0.4916	0.6001	5.7342	−5.7298	−2.7948	−0.1052	−1.7374	−1.7977
2	1.0705	−3.3675	1.2708	−0.8219	−2.9953	−2.018	8.1810	2.1016	−2.4561	−1.8507	
3	1.8841	1.4505	−1.6847	−4.1494	−1.6482	−2.4402	−0.2791	−2.8835	−1.2919	3.9722	
4	−1.0526	0.1461	0.8719	1.1347	2.0275	6.2501	0.1471	0.3680	−3.6188	5.6256	

AAD% between the experiment results[12] and the network with tansig function for 15 wt.% MDEA + 11 wt.% PZ, 18 wt.% MDEA + 12 wt.% MEA and 12 wt.% MDEA + 18 wt.% MEA was estimated as 4.81%. However, the AAD% of the experiment results and the network with the logsig function for these three solvents were determined as 5.61%. It was observed that, the deviation of high partial pressure region (>500 kPa) is larger than low pressure region (< 500 kPa), the lack of input data set related to high pressure region was the main possible reason. However, the experiment of this present research was investigated over the CO_2 partial pressure range between 8 and 100 kPa, meaning that both models A and B were able to predict the CO_2 solubility in the present work. Both figures above indicated that the average deviations of tansig and logsig function are strongly affected by the input parameters and there are some other possible factors can also affect the prediction results such as the number of neurons, the number of input parameters and number of hidden layers. It can be concluded that tansig function in multiple hidden layers provides better prediction accuracy than logsig function. Specifically, it was found that the deviation of using logsig function at high pressure region are higher. The possible reason is that the output values bound for tansig function can be normalizing from -1 to 1, meaning that it accepts larger output values bound than logsig function. For the logsig function, the gradient changes of the loading at high pressure are small, and it causes the network refusing to learn the data regarding the high pressure.

The determination of deviation between both two models and experimental results were subsequently
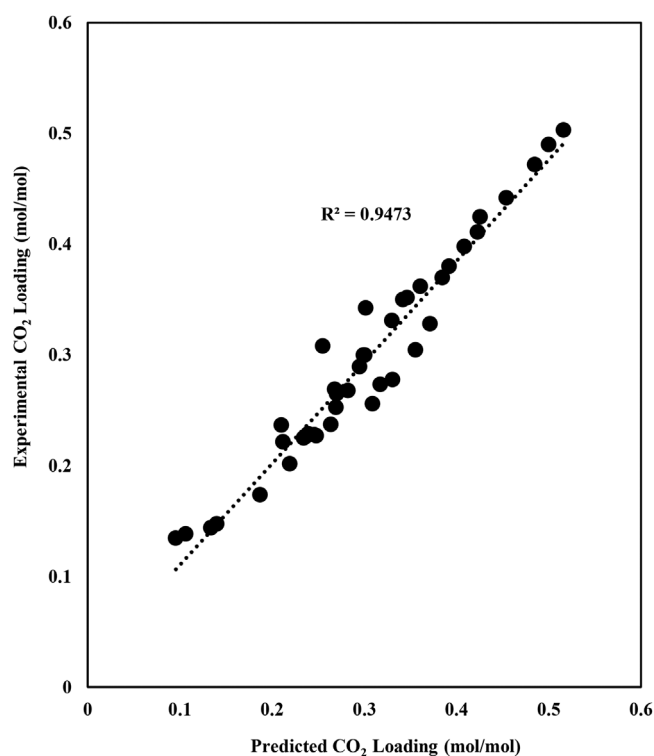
Figure 7. Correlation coefficient for model A.

provide the reliability of the models. The network configuration of the model A with tansig function as shown in Fig. 7, which gives an acceptable value of 0.9473 of R^2, 0.000654 of MSE and 8.4 of MRE. Therefore, the validation results showed that the network with two hidden layers consists of eight and four neurons provides predictions in acceptable agreement with the published experimental data. For the model B, the network configuration of model B
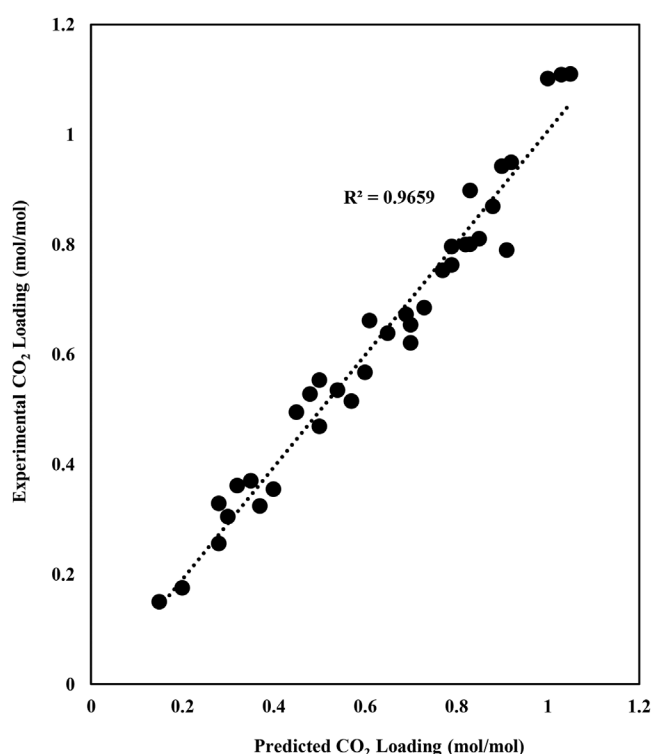
Figure 8. Correlation coefficient for model B.

gives an acceptable value of 0.9659 of R^2, 0.0023 of MSE, and 6.9 of MRE shown in Fig. 8. Tables 7–9 stated the weights and biases of model B, which consists of three hidden layers including 20, 10, and five hidden neurons in the first, second, and third hidden layers, respectively.

Experimental and validation results

The benchmark aqueous 30 wt.% MEA solution was investigated to validate the experiment was accurate and effective. A lot of experimental data related to CO_2 solubility in different concentration of MEA solvents have been published by several researchers. The experiment of this present research was implemented with the CO_2 partial pressure between 8 and 100 kPa, therefore the references of the experimental data were all obtained under the CO_2 partial pressure between 0 and 100 kPa.[38,48,49]

Figure 9 indicates a comparison of CO_2 solubility in 30 wt.% MEA between the published experimental data[38,48,49] and the results of this work. It was observed that the AAD% between the experimental data of this work and the experimental data reported by Shen *et al.*[48] was found as 1.2%, meaning the experimental results of this work are accurate and effective. However,

it was found that the AAD% between the simulation and the experiment is higher than 10% in the high CO_2 partial pressure region (>50 kPa). Thus, developing a high prediction accuracy model can help investigator to correlate and predict the experimental results.

In this research, the total amine concentrations of three blended amine samples were maintained at 5 ± 0.2 mol L^{-1}. Table 10 reflects the experimental results of the CO_2 solubilities at 40 °C in various aqueous blended amine solvents. It can be observed that the CO_2 loading increases when increasing CO_2 partial pressure. The CO_2 solubility in three amine blends are higher than 30 wt.% MEA., and 24 wt.% MDEA + 26 wt.% PZ provides the best CO_2 solubility ability among these solvents at 40°C. This phenomenon represents that adding PZ and MDEA into MEA can rapidly increase the CO_2 solubility due to the molecular structure of PZ. Unlike MEA, PZ contains two nitrogen atoms at opposite positions, the formation of PZ carbamate and PZ dicarbamate causes larger CO_2 absorption capacity with faster CO_2 absorption rate than MEA.

Simulation and modeling of CO_2 equilibrium solubility

Figures 10 and 11 clearly show the gradient of CO_2 loadings at different CO_2 partial pressure by using several measurement methods including experimental method, ANN method and rate-based simulation. Both figures can be divided as low-pressure zone (< 50 kPa) and high-pressure zone (>50 kPa). At low-pressure zone, the AAD% between the experiment results and ANN model for 36 wt.% MDEA + 17 wt.% PZ, 24 wt.% MDEA + 26 wt.% PZ, and 6 wt.% MEA + 24 wt.% MDEA + 17 wt.% PZ were estimated as 2.5, 4.8, and 3.5%, respectively. Also, the AAD% of the experiment results and simulations for 36 wt.% MDEA + 17 wt.% PZ, 24 wt.% MDEA + 26 wt.% PZ, and 6 wt.% MEA + 24 wt.% MDEA + 17 wt.% PZ were determined as 3.9, 8.4, and 2.6%, respectively. Once the CO_2 partial pressure greater than 50 kPa, the AAD% between the simulation predictions and ANN predictions for 36 wt.% MDEA + 17 wt.% PZ, 24 wt.% MDEA + 26 wt.% PZ, and 6 wt.% MEA + 24 wt.% MDEA + 17 wt.% PZ were estimated as 8.0, 10.6, and 11.6%, respectively. The increased deviation when increasing the concentration of PZ and pressure is mostly caused by nonideal phenomenon in the liquid phase due to the more complex interactions in a

Table 7. Weights and biases of model B for the first hidden layer.

Number of the neuron on the 1st hidden layer	Weight					
	X_{MEA}	X_{MDEA}	X_{PZ}	P_{CO2}	MWa	Bias
1	−1.3283	1.8805	−0.5962	−0.4747	−0.9719	2.4191
2	0.7139	1.5674	−1.5878	1.0016	0.4896	−2.2201
3	1.0899	−1.5448	0.0235	1.4014	−0.8634	−2.0316
4	−0.0056	−1.1859	0.1374	−1.4412	−0.7716	−2.3259
5	−1.0449	−1.5254	1.5854	0.2152	0.9068	1.2969
6	1.3299	−0.0522	1.1473	1.7695	0.4727	−1.1883
7	1.9112	−1.8596	−0.4971	−0.3413	0.2376	−0.4144
8	1.0714	1.6349	1.5397	−0.7979	0.4282	−0.7269
9	−1.4230	−1.3299	−1.2456	0.2295	−1.2443	0.6542
10	−0.7902	−2.1374	−7.0772	−0.3717	−0.9456	0.2662
11	1.0047	0.2931	2.0209	1.2515	−0.2233	0.0657
12	0.8899	1.0756	2.4022	−0.0202	−1.5591	0.4319
13	1.7611	−0.6424	1.3544	0.3246	1.9874	−0.4050
14	−1.5456	−1.5042	−0.3225	1.3956	1.6387	0.3877
15	0.0705	−0.3638	−0.0101	4.9961	−0.1688	4.5282
16	0.1947	−1.3045	2.0871	−0.5425	0.8229	−1.7506
17	0.6086	0.7097	−0.4087	4.3417	−0.6802	4.3703
18	−0.8936	1.4964	0.9513	1.0026	1.2817	−2.1052
19	−0.9963	0.3678	0.6751	1.1817	−1.3191	−2.4459
20	1.4492	−1.4851	1.9361	−1.3933	0.0847	2.0711

solvent. It is a relevant reason of ProMax slightly underpredicted or overpredicted the CO_2 solubility in amine blends. In ProMax, the phase behavior was modeled by the selected vapor and liquid model type. The simulated vapor-liquid equilibrium (VLE) data were achieved by employing Peng–Robinson Equation of State (EoS) to calculate the fugacity coefficient in the vapor phase and utilizing Electrolytic ELR to determine the activity coefficients in the liquid phase. Activity coefficients are the factors that affect the equilibrium constants rely on the amine concentration. ProMax, which is an accurate prediction tool in thermodynamics, thus has the ability to perform the reactions at equilibrium and predicting the equilibrium constants. However, uncertainties could occur for actual experiments. For example, there is a possibility that CO_2 partial pressure in the headspace is slightly less than in the feed gas when feeding a mixture of gases, which could slightly affect the final equilibrium CO_2 concentration. Hence, the predictions using ANN

were more accurate as shown in Figs. 10 and 11. The leading advantage of using neural network model as the prediction tool is that ANN models were developed by using real experimental data. ANN have strong ability to model complex nonlinear functions with high computation capacity, its large interpolation capacity contributes strong ability to accept and to generalize new data through training process. Two prediction methods both confirmed the experimental results that the absorption capacity could be ranked as 24 wt.% MDEA + 26 wt.% PZ > 6 wt.% MEA + 24 wt.% MDEA + 17 wt.% PZ > 36 wt.% MDEA + 17 wt.% PZ > 30 wt.% MEA.

Comparison of ANN and other published methods

To properly investigate the prediction accuracy for ANN models, a comparison study between ANN models and other thermodynamic models is certainly

Table 8. (a) Weights and biases of model B for the second hidden layer (part 1).

Number of the neuron on the 2nd hidden layer	Weight									
	Number of the neuron on the 1st hidden layer									
	1	2	3	4	5	6	7	8	9	10
1	−0.3273	−0.4745	0.0277	0.0552	0.4535	0.3369	−0.1179	0.3285	−0.1638	−0.3829
2	0.2809	0.0587	−0.2315	−1.8156	0.0314	0.0313	−0.5385	−0.8889	0.5865	0.1194
3	−0.0730	0.0504	−0.0638	0.3261	−0.2756	−0.1017	0.1128	−0.4867	0.3304	0.7444
4	0.0438	0.2458	−0.6931	−1.3072	−0.7546	0.0236	2.7386	1.5048	0.2755	0.5741
5	0.4565	−0.1199	−2.3102	−0.4826	3.2784	1.6781	−0.3275	−0.1720	0.2194	−0.1285
6	−0.2387	−0.0520	−0.2973	−0.09204	0.8835	0.0887	0.77934	0.9612	−0.2307	−0.3937
7	0.0483	0.3348	−0.2563	0.7411	0.3299	0.3573	0.1152	0.4874	−0.5938	0.3940
8	0.4663	−0.4333	−0.3348	0.4185	0.3738	−0.0031	−0.08703	−0.3216	−0.0036	0.5495
9	−0.5761	−0.3711	−0.0899	0.8496	−0.1425	0.0907	0.2374	0.2642	0.3253	0.4944
10	0.7601	0.5147	−0.5831	0.1898	−0.5125	0.0399	−0.0924	0.4289	0.1344	−0.2147

(b) Weights and biases of model B for the second hidden layer (part 2).

| Number of the neuron on the 2nd hidden layer	Weight									
	Number of the neuron on the 1st hidden layer									
	12	13	14	15	16	17	18	19	20	Biases
1	0.5724	−0.1607	−0.0556	1.5591	−0.2461	0.4479	−0.3247	0.3812	0.3812	1.7047
2	0.5449	1.1841	1.3787	5.2003	−0.3501	4.4323	−0.5152	−0.2289	0.0954	−0.8861
3	−0.6804	−0.1353	0.1780	0.7725	−0.6081	−1.5153	−0.3101	0.5457	0.1226	−1.0278
4	−0.1852	−1.7919	0.1083	−0.4402	0.4168	0.7273	−0.3814	0.0152	−0.3111	0.5910
5	−0.2296	0.5448	−0.2831	−0.3128	−0.0511	0.3464	−0.6363	0.0634	0.1595	−0.2141
6	0.9831	0.7474	1.2291	3.0424	−0.4627	2.2866	0.3748	−0.4302	1.5414	0.0532
7	0.5886	0.2152	0.5434	0.1512	−0.04487	−0.1386	−0.4302	−0.1242	0.3157	−0.4661
8	0.4951	−0.1317	0.3741	−0.077	−0.4902	−0.0077	0.4943	0.0916	0.4317	0.7993
9	−0.3986	−0.2518	−0.145	−1.9691	0.2083	−1.5036	−0.0884	−1.4727	5.05504	−1.3504
10	−0.2599	0.0322	0.0557	−0.6970	−1.0889	−1.2131	0.2976	0.3168	−0.4307	1.5819

beneficial. In this work, model A is proposed to predict the CO_2 solubility at temperature range from 303 to 393 K and CO_2 partial pressure from 0.06 to 4978 kPa, meaning it can efficiently cover the range of the experimental results reported by Vahidi *et al.*[37]

Vahidi *et al.*[37] applied a thermodynamic model proposed by Liu *et al.*[21] based on extended Debye–Hückel theory to correlate and predict the CO_2 solubility in MDEA/PZ blends at the temperature range between 313 and 343 K and CO_2 partial pressures ranging from 30 to 5000 kPa. Although the results received an acceptable average absolute relative deviation percentage of 8.11%, the comparison results indicated that the prediction accuracy were reduced when temperature was increased. Table 11 indicated the AAD% for three prediction models by comparing with the reliable experimental data reported by Vahidi *et al.*[37] It was found that both the thermodynamic

Table 9. Weights and biases of model B for the second hidden layer.

| Number of the neuron on the 3rd hidden layer | Weight | | | | | | | | | | | Output layer | |
| | Number of the neuron on the 2nd hidden layer | | | | | | | | | | | Weight | |
	1	2	3	4	5	6	7	8	9	10	Bias	α	Biases
1	0.8674	3.5839	0.2017	0.0375	0.7620	0.5491	0.6743	−0.0573	0.7682	0.2111	−1.6156	0.1303	−0.8316
2	−0.216	−0.6363	0.5437	−0.9489	0.6319	0.3632	0.3442	−0.5776	−0.5178	−0.6673	−0.6455	−0.1696	
3	0.5903	0.5086	1.6585	−0.2877	−0.0219	−0.126	−0.8874	−0.9537	0.5450	0.3941	−0.2259	−2.4889	
4	0.2411	−0.1793	−0.4306	0.7178	0.1121	0.5019	−0.5405	1.2513	−0.0222	0.3786	0.9823	−0.9964	
5	1.3098	6.7318	−0.6196	−0.0254	−0.3224	4.6262	0.0479	−0.7093	−2.5678	−1.4612	1.8053	3.2296	
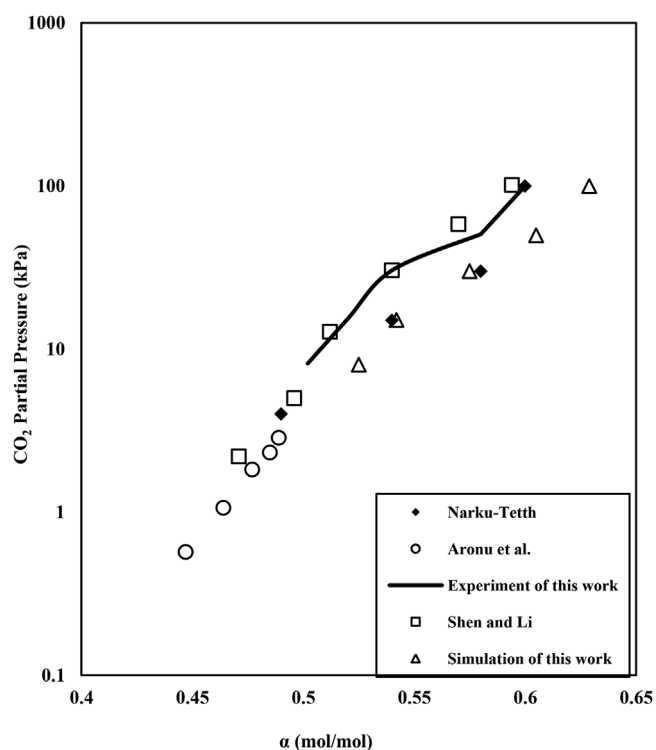
Figure 9. Validation of CO_2 solubility data for 30 wt.% MEA by comparison with literature works and simulation results.

Table 10. CO_2 Solubilities in blended aqueous solvents at 40 °C.

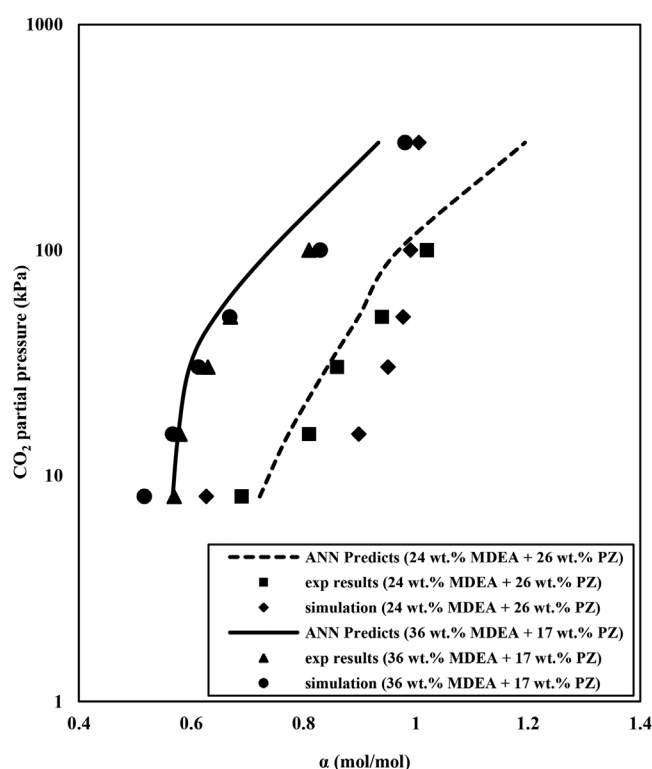| P_{CO2} (kPa)	α
6 wt.% MEA + 24 wt.% MDEA + 17 wt.% PZ	
8.1	0.59
15.3	0.61
30.4	0.66
50.65	0.710.82
100	
36 wt.% MDEA + 17 wt.% PZ	
8.1	0.57
15.3	0.58
30.4	0.63
50.65	0.670.81
100	
24 wt.% MDEA + 26 wt.% PZ	
8.1	0.69
15.3	0.81
30.4	0.86
50.65	0.941.02
100	

Figure 10. Experimental, simulated, and ANN (model A) predicted CO_2 solubility in aqueous 36 wt.% MDEA + 17 wt.% PZ and 24 wt.% MDEA + 26 wt.% PZ.
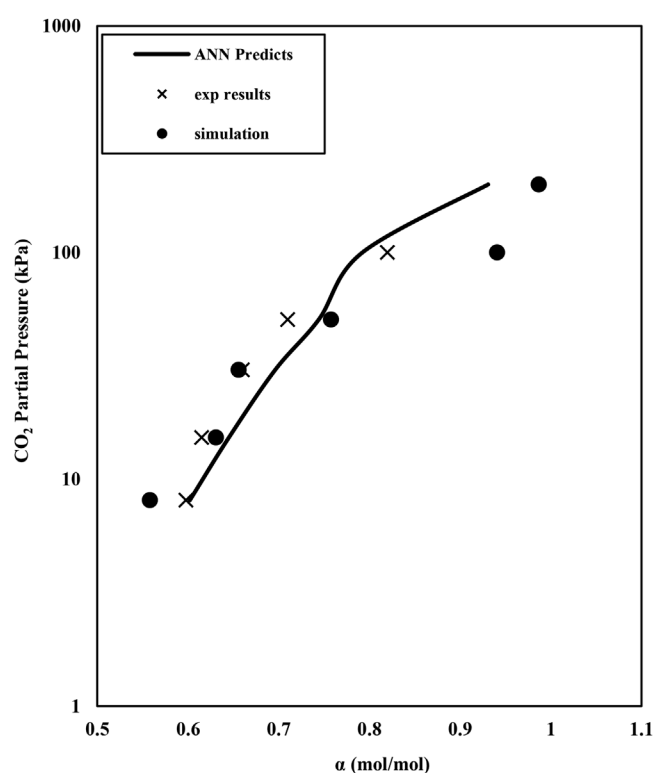

Figure 11. Experimental, simulated, and ANN (model B) predicted CO_2 solubility in aqueous 6 wt.% MEA + 24 wt.% MDEA + 17 wt.% PZ.

model based on extended Debye–Hückel theory and ANN model were able to predict CO_2 solubility in 24 wt.% MDEA + 12 wt.% PZ and 30 wt.% MDEA + 7 wt.% PZ accurately, since the AADs are all less than 10%. Figs.12 and 13 illustrated the comparison of the CO_2 loadings at different CO_2 partial pressures for 24 wt.% MDEA + 12 wt.% PZ and 30 wt.% MDEA + 7 wt.% PZ, respectively. P_{cal1} represents the calculated CO_2 partial pressure by using the thermodynamic model based on extended Debye–Hückel theory reported by Vahidi e*t al.*[37] P_{cal2} represents the calculated CO_2 partial pressure by using the model proposed by Liu *et al.*[21] calculated by Vahidi *et al.*;[37] P_{ann} represents the predicted CO_2 partial pressure by using model A proposed in this work; P_{exp} represents the experimental data reported by Vahidi *et al.*[37] It was observed that the deviations between the Liu. H.B model and experimental data reported by Vahidi *et al.*[37] in high CO_2 partial pressure region (>500 kPa) are significantly higher than other two prediction methods. Among the three models, model A in this work provides the best performance in predicting the CO_2 solubility in 24 wt.% MDEA + 12

Table 11. Comparison of predicted CO_2 partial pressure with different methods for CO_2 solubility in different amine solvents.

| | | AAD% | | |
Amine	Temperature (K)	Liu's model[37]	ED-H model[37]	Model A[a]
24 wt.% MDEA + 12 wt.% PZ	313.15	15.65	4.21	2.3
	328.15	82.56	7.76	6.18
	343.15	47.5	8.23	3.04
30% wt.% MDEA + 7 wt.% PZ	313.15	19.21	6.08	3.33
	328.15	33.44	9.95	2.38
	343.15	23.1	10.22	9.78

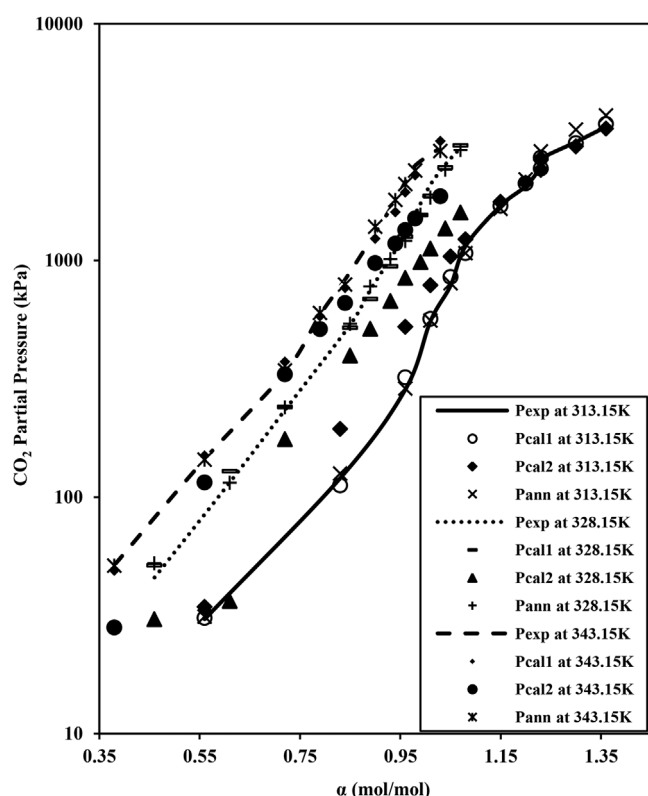[a]Predictions from Model A of this work

Figure 12. Comparison of prediction performance for CO_2 solubility in 24 wt.% MDEA + 12 wt.% PZ between model A and other models proposed by Vahidi *et al*.[37] and Liu *et al*.[21] using experimental data reported by Vahidi *et al*.[37]
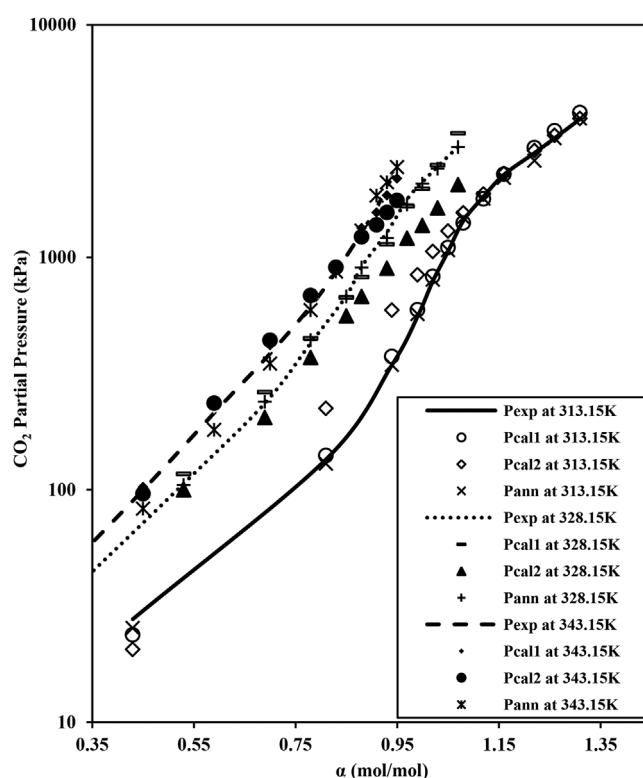

Figure 13. Comparison of prediction performance for CO_2 solubility in 20 wt.% MDEA + 7 wt.% PZ between model A and other models proposed by Vahidi *et al*.[37] and Liu *et al*.[21] by using the experimental data reported by Vahidi *et al*.[37]

wt.% PZ and 30 wt.% MDEA + 7 wt.% PZ. Model A comprised of a large number of neurons, each of them supports the system to have a simple decision and be closer to the desired output. Therefore, the network is able to learn and extract relevant information to predict appropriate loadings by connecting each neuron. Furthermore, model A was trained by using backpropagation theory, which helps the network to learn backward due to the existence of its derivative function and understand which weights in the input neurons can predict more accurate outputs. It is known that the prediction accuracy of the network with linear activation functions will be reduced if the model is too complex, because the last layer will always be a linear function with the first layer. Therefore, the network with linear function cannot accept backpropagation training function and it turns the network into one layer no matter how many hidden layers exist.[57] Unlike linear activation functions, nonlinear activation function helps model A accepts multilayers structure to

handle the input data of the work and it improves the data processing capabilities.

The model of Kent and Eisenberg was used to predict the solubilities of CO_2 in blended MEA/MDEA solvent by Li and Shen.[58] They obtained several groups of data regarding the CO_2 solubility in 24 wt.% MDEA + 12 wt.% MEA at different temperatures.[59] It was mentioned that model B was trained under 40 °C. It can therefore be used to compare the accuracy with the predictions by using the model of Kent and Eisenberg as shown in Fig. 14. The average deviation of the prediction between model B and the published experimental data is 6.59%,[59] which is slightly lower than using the Kent and Eisenberg model (7.01%). The high deviation appears below 1 kPa due to the lack of data regarding the mixture of MDEA/MEA below 1 kPa. This is because the normalizing output is extremely close. However, the results still acceptable because the model A is closer to the Austen's experimental data.[59] According to Figs. 13 and 14, it can be concluded that the predictions of ANN models
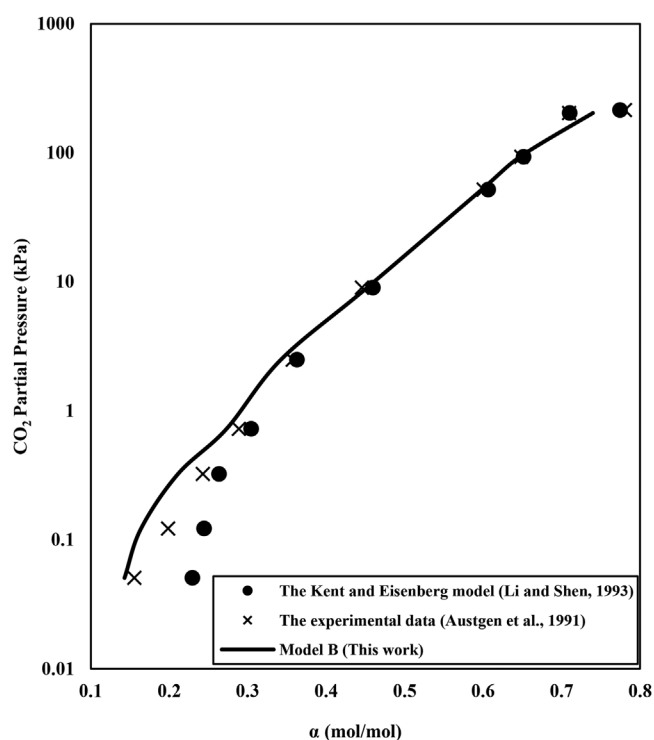
Figure 14. Comparison of prediction performance for CO_2 solubility in 24 wt.% MDEA +12 wt.% MEA between model B in this work and the Kent and Eisenberg model[58] using experimental data reported by Austen *et al*.[59]

are in good agreements with actual CO_2 solubility data and exhibit better results than other models.

Conclusions

CO_2 solubility is investigated experimentally for evaluating the CO_2 absorption performance in aqueous blended amine solutions of MDEA/PZ and MEA/MDEA/PZ. The performance can be ranked as 24 wt.% MDEA + 26 wt.% PZ > 6 wt.% MEA + 24 wt.% MDEA + 17 wt.% PZ > 36 wt.% MDEA + 17 wt.% PZ > 30 wt.% MEA at CO_2 partial pressure from 8 to 100 kPa and temperature of 40 °C. It can be concluded that CO_2 solubility is a physical property that is strongly affected by the temperature, pressure, solvent concentration, and solvent type. One of the main advantages of the desired neural network model is high data reliability. The network is trained based on the reliable experimental data, and efficiently computing input data to output data through nonlinear relationship functions. This work confirmed that the network with two hidden layers using eight and four neurons provides high prediction accuracy on CO_2

solubility for bi-solvent when using four input parameters. Model A proposed in this work can efficiently predict CO_2 solubility in various concentration of the MDEA/PZ blends at a wide range of CO_2 partial pressure from 0.06 to 4978 kPa at the temperature range between 303 and 393 K. Tri-solvents are normally regarded as more complicated chemical structures than bi-solvents. Therefore, a new network architecture is proposed to obtain a higher prediction accuracy on CO_2 solubility in tri-solvents containing five input parameters and three hidden layers using 20, 10, and five neurons in the first, second, and third hidden layer, respectively. It should be mentioned that model B can be developed in a wide range of temperature once the reliable experimental data are abundant. Two developed ANN models can both provide satisfying prediction performance in predicting the CO_2 solubility.

Nomenclature

P_{CO2}	CO_2 partial pressure, kPa
T	Operating temperature, K or °C
X	The overall concentration of the amine in the solvent, wt.%
X_{MEA}	Weight fraction of MEA, wt.%
X_{MDEA}	Weight fraction of MDEA, wt.%
X_{PZ}	Weight fraction of PZ, wt.%
MW_a	Apparent molecular weight, g mol^{-1}
MEA	Monoethanolamine
MDEA	Methyldiethanolamine
PZ	Piperazine
CO_2	Carbon dioxide
Y_i	the normalized training and testing data sets
Xi	the training and testing data sets
X_{min}	the minimum values of variable
X_{max}	the maximum values of variable
AAD%	absolute average deviation, %
R^2	The correlation coefficient
MSE	The mean square errors
MRE	The mean relative errors
exp	Experimental data

Symbol

$\alpha\ CO_2$ loading, mol_{CO2}/mol_{amine}

Conflict of Interest

The authors declare no competing financial interest.

References

1. IEA, *World Energy Outlook 2020 Part of World Energy Outlook*. IEA Publications, Pairs, France (2020).

2. EIA, *International Energy Outlook*. U.S. Department of Energy, Washington, DC (2016).

3. Lockwook T, A comparative review of next-generation carbon capture technologies for coal-fired power plant. *Energy Procedia* **114**:2658–2670 (2017).

4. GlobalCCS Institute, *Global Status of CCS 2020*. Global CCS Institute, Docklands, Australia (2020)

5. Putta KR, Svendsen HF and Knuutila HK, Kinetics of CO_2 absorption in to aqueous MEA solutions near equilibrium. *Energy Procedia* **114**:1576–1583 (2017).

6. Gunasekaran P, Veawab A and Aroonwilas A, Corrosivity of amine-based absorbents for CO_2 capture. *Energy Procedia* **114**:2047–2054 (2017).

7. Luis P, Use of monoethanolamine (MEA) for CO_2 capture in a global scenario: Consequences and alternatives. *Desalination* **380**:93–99 (2016).

8. Moioli S and Pellegrini LA, Physical properties of PZ solution used as a solvent for CO_2 removal. *Chem Eng Res Des* **93**:720–726 (2015).

9. Liu H, Chan C, Tontiwachwuthikul P and Idem R, Analysis of CO_2 equilibrium solubility of seven tertiary amine solvents using thermodynamic and ANN models. *Fuel* **249**:61–72 (2019).

10. Nwaoha C, Supap T, Idem R, Saiwan C, Tontiwachwuthikul P, Al-Marri M *et al*., Advancement and new perspectives of using formulated reactive amine blends for post-combustion carbon dioxide (CO_2) capture technologies. *Petroleum* **3**:10–36 (2016).

11. Moioli S and Pellegrini LA, Modeling the methyldiethanolamine-piperazine scrubbing system for CO_2 removal: Thermodynamic analysis. *Front Chem Sci Eng* **10**(1):162–175 (2016).

12. Rayer A, Sumon KZ, Sema T, Henni A, Idem R and Tontiwachwuthikul P, Solubility of CO_2 in reactive solvents for post-combustion CO_2 capture, in *Recent Progress and New Development Post-Combustion Technology with Reactive Solvents* ed. by Tontiwachwuthikul P and Idem I. Future Science, London, UK (2013)

13. Chen, G, Wang X, Liang Z, Gao R, Sema T, Luo P *et al*., Simulation of CO_2 -oil minimum miscibility pressure (MMP) for CO_2 enhanced oil recovery (EOR) using neural networks. *Energy Procedia* **37**:6877–6884 (2013).

14. Molina CT and Bouallou C, Kinetics study and simulation of CO_2 absorption into mixed aqueous solutions of methyldiethanolamine and diethanolamine. *Chem Eng Trans* **35**: 319–324 (2013).

15. Kim D, Shi H and Lee JY, CO_2 absorption mechanism in amine solvents and enhancement of CO_2 capture capability in blended amine solvent. *Int J Greenhouse Gas Control* **45**:181–188 (2016).

16. Idem R, Edali M and Aboudheir A, Kinetics, modeling, and simulation of the experimental kinetics data of carbon dioxide absorption into mixed aqueous solutions of MDEA and PZ using laminar jet apparatus with a numerically solved absorption-rate/kinetic model. *Energy Procedia* **1**:1343–1350 (2009).

17. Santos SP, Gomes JF and Bordado J, Scale-up effects of CO_2 capture by methyldiethanolamine (MDEA) solutions in terms of loading capacity. *Technologies* **4**(3):19 (2016).

18. Bishnoi S and Rochelle GT, Absorption of carbon dioxide into aqueous piperzine: Reaction kinetic, mass transfer and solubility. *Chem Eng Sci* **55**:5531–5543 (2000).

19. Derks PWJ, Carbon dioxide absorption in piperazine activated n-methyldiethanolamine. PhD Thesis. University of Twente, The Netherlands (2016).

20. Zhang R, Zhang X, Yang Q, Yu H, Liang Z and Luo X, Analysis of the reduction of energy cost by using MEA-MDEA-PZ solvent for post-combustion carbon dioxide capture (PCC). *Appl Energy* **205**:1002–1011 (2017).

21. Liu HB, Zhang CF and Xu GW, A study on equilibrium solubility for carbon dioxide in methyldiethanolamine-piperazine-water solution. *Ind Eng Chem Res* **38**:4032–4036 (1999).

22. Khan S, Hallegiorgis SM, Man Z and Shariff AM, Solubility of CO_2 in piperazine activated aqueous n-methyldiethanolamine (MDEA) solvent under high pressure. *J Adv Res Fluid Mechanics Thermal Sci* 2289-7879 (2018).

23. Inoue S, Itakura T, Nakagaki T, Furukawa Y, Sato H, and Yamanaka Y, Experimental study on CO solubility in aqueous piperazine/alkanolamines solutions at stripper conditions. GHGT-11. *Energy Procedia* **37**:1751–1759 (2013).

24. Ali BS and Aroua MK, Effect of piperazine on CO_2 loading in aqueous solutions of MDEA at low pressure. *Int J Thermophys* **25**(6):1863–1870 (2004).

25. Dash SK and Bandyopadhyay S, Studies on the effect of addition of piperazine and sulfolane into aqueous solution of N-methyldiethanolamine for CO_2 capture and VLE modelling using eNRTL equation. *Int J Greenhouse Gas Control* **44**:227–237 (2016).

26. Sipocz N, Tobiesen FA and Assadi M, The use of artificial neural network models for CO_2 capture plants. *Appl Energy* **88**: 2368–2376 (2016).

27. Tatar A, Barati A, Yarahmadi A, Najafi A, Lee M and Bahadori A, Prediction of carbon dioxide solubility in aqueous mixture of methyldiethanolamine and N-methylpyrrolidone using intelligent models. *Int J Greenhouse Gas Control* **47**: 122–136 (2016).

28. Chan V and Chan C, Learning from a carbon dioxide capture system dataset: application of the piece wise neural network algorithm. *Petroleum* **3**(1):56-67 (2017).

29. Xia L, Wang J, Liu S, Li Z and Pan H, Prediction of CO_2 solubility in ionic liquids based on multi-model fusion method. *Processes* **7**(5):258 (2019).

30. Garg S, Shariff AM, Shaikh MS, Lal B, Suleman H and Faiqa N, Experimental data, thermodynamic and neural network modeling of CO_2 solubility in aqueous sodium salt of L-phenylalanine. *J CO2 Util* **19**:146–156 (2017).

31. Hamzehie ME and Najibi H, Prediction of acid gas solubility in amine, ionic liquid and amino acid salt solutions using artificial neural network and evaluating with new experimental measurements. *J Nat Gas Sci Eng* **29**:252–263 (2016).

32. Svozil D, Kvasncka V and Pospichal J, Introduction to multilayer feed-forward neural networks. *Chemom Intell Lab Syst* **39**:43-62 (1997).

33. Li H, Yan D, Zhang Z and Lichtfouse E, Prediction of CO_2 absorption by physical solvents using a chemoinformatics-based machine learning model. *Environ Chem Lett* **17**(3):1397–1404 (2019).

34. Okoye C, Carbon dioxide solubility and absorption rate in monoethanolamine/piperazine/H_2O. Master thesis. The University of Texas at Austin, TX (2005).

35. Austgen DM, Rochelle GT and Chen CC, Model of vapor-Liquid Equilibria for aqueous acid gas – alkanolamine systems. 2. Representation of H_2S and CO_2 solubility in aqueous MDEA and CO_2 solubility in aqueous mixtures of MDEA with MEA or DEA. *Ind Eng Chem Res* **30**:543–555 (1991).

36. Li MH and Shen KP, Densities and solubilities of solutions of carbon dioxide in water+monoethanolamine + n-methyldiethanolamine. *J Chem Eng Data* **37**:288–290 (1992).

37. Vehidi M, Matin NS, Goharrokhi M, Jenab MH, Abdi MA and Najibi SH, Correlation of CO_2 solubility in n-methyldiethanolamine + piperazine aqueous solutions using extended debye-huckel model. *J Chem Thermodynamics* **41**:1272–1278 (2009).

38. Narku-Tetteh J, Development of criteria for selection of components for formulation of amine blends based on structure and activity relationships of amines, and validation of formulated blends in a bench scale CO_2 capture pilot plant. Master of Process Systems. Engineering Thesis. University of Regina, Saskatchewan, Canada (2017).

39. Fotoohi F, Amjad-Iranagh S, Golzar K and Modarress H, Predicting pure and binary gas adsorption on activated carbon with two-dimensional cubic equations of state (2-D EOSs) and artificial neural network (ANN) method. *Phys Chem Liq* **54**(3): 281–302 (2016).

40. Garg S, Shariff AM, Shaikh MS, Lal B, Suleman H and Faiqa N, Experimental data, thermodynamic and neural network modeling of CO_2 solubility in aqueous sodium salt of L-phenylalanine. *J CO2 Util* **19**:146–156 (2017).

41. Baghban A, Ahmadi MA and Shahraki BH, Prediction carbon dioxide solubility in presence of various ionic liquids using computational intelligence approaches. *JSupercrit Fluids* **98**:50–64 (2015).

42. Fu K, Chen G, Liang Z, Sema T, Idem R and Tontiwachwuthikul P, Analysis of mass transfer performance of monoethanolamine-based CO_2 absorption in a packed column using artificial neural networks. *Ind Eng Chem Res* **53**(11):4413–4423 (2014).

43. Pouryousefi F, Idem R, Supap T and Tontiwachwuthikul P, Artificial neural networks for accurate prediction of physical properties of aqueous quaternary systems of carbon dioxide (CO_2)-loaded 4-(Diethylamino-2-butanoll and methyldiethanolamine blended with monoethanolamine. *Ind Eng Chem Res* **55**(44):11614–11621(2015).

44. Chen G, Luo X, Zhang H, Fu K, Liang Z, Rongwong W *et al*., Artificial neural network models for the prediction of CO_2 solubility in aqueous amine solutions. *Int J Greenhouse Gas Control* **39**:174–184 (2015).

45. Hamzehie ME, Mazinani S, Davardoost F, Mokhtare A, Najibi H Van der Bruggen B *et al*., Developing a feed forward multilayer neural network model for prediction of CO_2 solubility in blended aqueous amine solutions. *J Nat Gas Sci Eng* **21**:19–25 (2014).

46. Golzar K, Modarress H and Amjad-Iranagh S, Evaluation of density, viscosity, surface tension and CO_2 solubility for single, binary and ternary aqueous solutions of MDEA, PZ and 12 common ILs by using artificial neural network (ANN) technique. *Int J Greenhouse Gas Control* **53**:187–197 (2016).

47. Dorofki M, Elshafie AH, Jaafar O, Karim OA and Mastura S, Comparison of Artificial Neural Network Transfer Functions abilities to simulate extreme runoff data. *Proceedings of the 2012 International Conference on Environment, Energy and Biotechnology, Kuala Lumpur, Malaysia*. (2012).

48. Shen KP and Li MH, Solubility of carbon dioxide in aqueous mixtures of monoethanolamine with methyldiethanolamine. *J Chem Eng Data* **37**:96–100 (1992).

49. Aronu UE, Gondal S, Hessen ET, Warberg TH, Hartono A, Hoff KA *et al*., Soubility of CO_2 in 15,30,45 and 60 mas% MEA from 40 to 120°C and model representation using the extended UNIQUAC framework. *Chem Eng Sci* **66**:6393–6406 (2011).

50. Dang H, CO_2 absorption rate and solubility in monoehanolamine/piperzine/water. Master Thesis. University of Texas at Austin (2001)

51. Derks PWJ, Carbon dioxide absorption in piperazine activated n-methyldiethanolamine. PhD Thesis. University of Twente, The Netherlands (2006).

52. Singh P, Amine based solvent for CO_2 absorption "From molecular structure to process." Thesis, University of Twente, The Netherlands (2011).

53. Kadiwala S, Rayer AV and Henni A, High pressure solubility of carbon dioxide (CO_2) in aqueous piperazine solutions. *Fluid Phase Equilib* **292**:20–28 (2010).

54. Hamidi R, Farsi M and Eslamloueyan R, CO_2 solubility in aqueous mixture of MEA, MDEA and DAMP: Absorption capacity, rate and regeneration. *J Mol Liq* **265**:711–716 (2018).

55. Huang J, Gong M, Dong X, Li X and Wu J, CO_2 solubility in aqueous solutions of N-methyldiethanolamine+piperzine by electrolyte NRTL model. *Science China* **59**:360–369 (2016).

56. Ermatchkov V, Kamps PA, Speyer D and Maurer G, Solubility of carbon dioxide in aqueous solutions of piperazine in the low gas loading region. *J Chem Data* **5**:1060–1073 (2006).

57. Wang Y, Li Y, Song Y and Rong X, The influence of the activation function in a convolution neural network model of facial expression recognition. *Appl Sci* **10**: 1897 (2020).

58. Li MH and Shen K, Calculation of quilibrium solubility of carbon dioxide in aqueous mixtures of monoethanolamine with methyldiethanolamine. *Fluid Phase Equilib* **85**:129–140 (1993).

59. Austgen DM, Rochelle GTm and Chen C, Model of vapor liquid equilibria for aqueous acid gas-alkanolamine systems. 2. Representation of H_2S and CO_2 solubility in aqueous MDEA and CO_2 solubility in aqueous mixtures of MDEA with MDEA or DEA. *Ind Eng Chem Res* **30**(3):543–555 (1991).
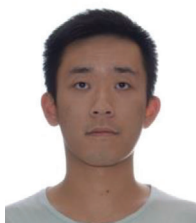
Tianci Li

Tianci is currently a first-year doctoral student in process systems engineering at the University of Regina, working under Dr Paitoon Tontiwachwuthikul's supervision as an engineer in training. He completed his master's degree in process systems engineering, and the topic of his thesis is 'A Comparison Study of Carbon Dioxide Absorption Performance in MEA and Blended Amine Solvents for Post-combustion Process: Experiment, Modeling and Simulation.' Before that, he achieved a BASc in petroleum engineering from the University of Regina. His major research interests are the CO_2 capture process, heat and mass transfer phenomena with chemical reactions, process simulation and modeling, machine learning, and neural networks applied to current CO_2 capture industry. He is also a graduate teaching assistant for several undergraduate and graduate level chemical engineering classes and labs.

Puttipong Tantikhajorngosol

Dr Tantikhajorngosol is a postdoctoral researcher, graduated in 2018. He holds a BSc in chemistry (2006), a MSc in chemical engineering (2010), and a PhD in energy technology (2018) from King Mongkut's University of Technology Thonburi (Thailand). His research interests cover membrane technologies, thermodynamics, mass transfer, modeling, and process simulation applied to CO_2 capture and gas separation processes of both natural gas and biogas.

Paitoon Tontiwachwuthikul

Dr Paitoon Tontiwachwuthikul (known as P.T.), is currently a full professor and the cofounder of Clean Energy Technology Research Institute (CETRi) at the University of Regina. Dr P.T. obtained his PhD degree in chemical engineering from University of British Columbia (UBC) in 1991. Dr P.T. is a key international researcher in the area of advanced CO_2 capture and separation from industrial gas streams as well as low-carbon energy development. He has provided technical advice to governments and industries nationally and internationally. Dr PT has played a vital role in the establishment of the Petroleum Technology Research Centre (PTRC), one of the largest petroleum research centers in North America. He has also served as a guest editor of the IEAGHG special issue on 'IEA Weyburn–Midale CO_2 Monitoring and Storage Project (the world largest CO_2 for EOR and CCS program)' in *International Journal of Greenhouse Gas Control* (IJGGC Elsevier), in 2013. Dr P.T. is currently a member of Editorial Board of IJGGC (Elsevier) and *Clean Energy Journal* (Oxford Press). In addition he is serving as the honorary editor-in-chief of *PETROLEUM Journal* (Elsevier). Dr P.T. has published extensively in *AIChE Journal*, *Applied Energy*, *Fuels*, *Chemical Engineering Science*, *International Journal of Greenhouse Gas Control*, *Membrane Science*, *Petroleum*, *Chemical Engineering Journal*, *Carbon Management*, *Separation & Purification Technology*, *Petroleum*, *Engineering Applications of Artificial Intelligence*, and *Industrial & Engineering Chemistry Research*. His recent publications can be tracked in Google Scholar Citations: http://scholar.google.ca/citations?user=7sB0sckAAAAJ&hl=en

Congning Yang

Congning is presently a PhD student in process systems engineering at the University of Regina. She achieved a BASc degree in petroleum systems engineering in 2019 and she joined Dr Paitoon Tontiwachwuthikul's research group and received MASc degree in process systems engineering in 2020. Her research interest is carbon capture, storage and utilization technologies, greenhouse gas control technologies, thermodynamic modeling, heat and mass transfer with chemical reactions and membrane separation.